Evidence for the Formation of an Interstellar Species, HCS^+, during the Ionic Fragmentation of Methyl Thiofluoroformate, $FC(O)SCH_3$, in the 100−1000 eV Region

Mariana Geronés,[†] Mauricio F. Erben,[†] Rosana M. Romano,[†] Reinaldo L. Cavasso Filho,[‡] and Carlos O. Della Védova*[,†,§]

CEQUINOR (CONICET-UNLP), Departamento de Química, Facultad de Ciencias Exactas, Universidad Nacional de La Plata, C.C. 962 (1900) La Plata, República Argentina, Universidade Federal do ABC, Rua Catequese, 242, CEP: 09090-400, Santo André, São Paulo, Brazil, and Laboratorio de Servicios a la Industria y al Sistema Científico, LaSeISiC (UNLP-CIC−CONICET), Camino Centenario e/505 y 508, (1903) Gonnet, República Argentina

Received: August 26, 2010; Revised Manuscript Received: September 20, 2010

Total ion yield spectra and photoinduced fragmentations following S 2p, C 1s, O 1s, and F 1s inner shell excitations of methyl thiofluoroformate, $FC(O)SCH_3$, have been studied in the gaseous phase by using synchrotron radiation and multicoincidence techniques, which include photoelectron−photoion coincidence (PEPICO) and photoelectron−photoion−photoion coincidence (PEPIPICO) time-of-flight mass spectrometry. Fragmentation patterns deduced from PEPICO spectra at the various excitation energies show a moderate site-specific fragmentation. The dissociation dynamic for the main ion-pair production has been discussed. Two-, three-, and four-body dissociation channels have been observed in the PEPIPICO spectra, and the dissociation mechanisms were proposed. The high stability of the interstellar HCS^+ ion can be observed over the whole range of photon energies analyzed.

Introduction

Our research group has quite recently started studies concerning the electronic properties of shallow- and inner-core levels in sulfenylcarbonyl compounds with general formula XC(O)SCl. Thus, FC(O)SCl,[1,2] ClC(O)SCl,[3] $CH_3C(O)SH$,[4] and $CH_3OC(O)SCl$[5] species have been studied by using synchrotron radiation in the 100−1000 eV range, and their ionic fragmentations after electronic decay have been analyzed. Other sulfur-containing compounds, such as CH_3SCN and CCl_3SCl were also studied.[6,7] Very recently, we have succeeded in analyzing the electronic structure and the ionic dissociation induced by photon absorption in the outermost valence region of sulfenylcarbonyl compounds by using a combined experimental approach that includes HeI photoelectron spectroscopy and photoionization under the action of synchrotron radiation in the 12−21.5 eV region.[8−10]

The branching ratios for ion productions obtained from the PEPICO spectra of FC(O)SCl and ClC(O)SCl molecules exhibit only small changes with the incident photon energy,[1−3] which was interpreted in terms of a "lose memory" effect or nonspecific fragmentation after an Auger decay, promoted by the delocalization of valence orbitals over the whole planar molecules. On the other hand, a similar experimental study carried out for thioacetic acid, $CH_3C(O)SH$, was interpreted in terms of a moderate site-specific fragmentation evidenced by a diminution of the CH_3CO^+ fragment signal in going from the S 2p to the O 1s transition regions.[4] In the last molecule analyzed, $CH_3OC(O)SCl$, the PEPICO spectra reveal a preferential production of S^+ ions in the S 2p absorption edge that would seem to be evidence for state-specific fragmentations. Ionic double coincidences were also examined, and dissociation mechanisms were proposed to explain the shape and slope of observed PEPIPICO islands.[5]

In view of the rich photodissociation processes following the shallow- and core−shell electronic excitation displayed by sulfenylcarbonyl compounds, the extension of the study to another member of this family can be interesting. Thus, the main goal of the present study is to obtain evidence regarding the electronic transitions throughout the whole region of the S 2p, C 1s, O 1s, and F 1s core edges as well as the ionic dissociation mechanisms following the electronic relaxation of the core excited methyl thiofluoroformate, $FC(O)SCH_3$. The methodology includes the use of multicoincidence mass spectroscopy techniques and tunable synchrotron radiation. Fragmentation patterns deduced from PEPICO spectra at various excitation energies in the vacuum ultraviolet and soft X-ray regions were especially analyzed in order to establish the existence of a site-specific or state-specific fragmentation effect. In fact, differences in relative yields of fragment ions were observed in simple molecules by exciting K shell electrons.[11] The tunable synchrotron radiation can excite selectively inner shell electrons, and in a case where the memory effect induced on the short time scale of the excitation is conserved at longer times than that required for the ionic dissociation, nonstatistical fragmentations, i.e., site- and element-specific fragmentations, can be anticipated. The insight on the nature of the site specific fragmentation is of importance in understanding localization phenomena in chemical reactions.[12−16]

Relevant studies have been reported for the title molecule. Thus, its molecular structure has been early determined by a study of the microwave spectrum by Caminati and Meyer.[17] The syn conformation (in which the C═O bond is oriented syn with respect to the S−CH_3 bond), was deduced for the main conformer. The IR spectrum of $FC(O)SCH_3$, both as a vapor and trapped in a solid Ne or Ar matrix together with the Raman spectrum in the liquid phase, has already been reported.[18] These

* To whom correspondence should be addressed.
[†] CEQUINOR (CONICET-UNLP), Departamento de Química, Facultad de Ciencias Exactas, Universidad Nacional de La Plata.
[‡] Universidade Federal do ABC.
[§] Laboratorio de Servicios a la Industria y al Sistema Científico, LaSeISiC (UNLP-CIC−CONICET).

10.1021/jp1081164
Published on Web 10/28/2010

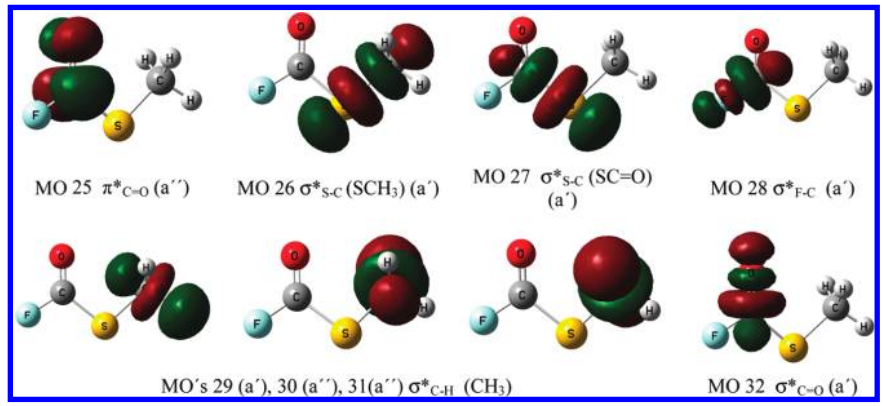

Figure 1. Schematic representation of the eight lower energy unoccupied molecular orbitals for $FC(O)SCH_3$ calculated at the B3LYP/6-311++G (d,p) level of approximation.

studies agree with the fact that the most abundant conformation is syn, at least at room temperature, and at a 95% concentration or higher. Moreover, the broad band UV−visible irradiation of $FC(O)SCH_3$, isolated in a solid Ar matrix at 15 K, has been investigated. Thus, in the first place the photoisomerization of the syn into the anti form of the molecule occurs, and, subsequently, the elimination of CO with the concomitant formation of CH_3SF is observed. Continued irradiation brings about tautomerization of this product with the detachment and migration of a hydrogen atom from the methyl group forming a $H_2C{=}S\cdots HF$ molecular complex.[19]Moreover, a SCH_3 containing molecule as $FC(O)SCH_3$ represents another good candidate to search for the formation of the HCS^+ interstellar species.

Experimental and Computational Methods

Synchrotron radiation was used at the Laboratório Nacional de Luz Síncrotron (LNLS), Campinas, São Paulo, Brazil.[20−22] Linearly polarized light monochromatized through a toroidal grating monochromator (available at the TGM beamline in the range 12−300 eV),[23,24] with resolving power of $\Delta E/E < 400$, to excite the region of S 2p, and a spherical grating monochromator (available at the SGM beamline in the range 200−1000 eV)[25] with $\Delta E/E < 200$, to excite the region of C 1s, O 1s, and F 1s, intersects the effusive gaseous sample inside a high vacuum chamber, with base pressure in the range 10^{-8} mbar. During the experiments the pressure was maintained below 2×10^{-6} mbar. The intensity of the emergent beam was recorded with a light-sensitive diode. The ions produced by the interaction of the gaseous sample with the light beam were detected using a time-of-flight (TOF) mass spectrometer of the Wiley−McLaren type for both PEPICO and PEPIPICO measurements.[26−28] This instrument was constructed at the Institute of Physics, Brasilia University, Brasilia, Brazil.[29] The axis of the TOF spectrometer was perpendicular to the photon beam and parallel to the plane of the storage ring. Electrons were accelerated to a multichannel plate (MCP) and recorded without energy analysis. This event starts the flight time determination process of the corresponding ion, which is consequently accelerated to another MCP.

The sample of methyl thiofluoroformate, $FC(O)SCH_3$ was prepared by the reaction between $ClC(O)SCH_3$ (Aldrich, estimate purity better than 95%) and TlF. The liquid was purified by repeated fractional condensation at reduced pressure in order to eliminate volatile impurities. The final purity of the compound in both the vapor and the liquid phases was carefully checked by IR and Raman spectroscopy.

Results and Discussion

Theoretical Calculations. It is well-established that the molecule of $FC(O)SCH_3$ in its electronic ground state belongs to the C_S symmetry point group. It follows that all the canonical molecular orbitals of type a′ are σ-orbitals lying in the molecular plane, while those of type a″ are π-orbitals. Accordingly, the ground state independent particle electronic configuration of methyl thiofluoroformate the 30 valence electrons are then arranged in 15 double-occupied Kohn−Sham orbitals (from now on orbital will be used as a colloquial denomination) in the independent particle description. The DFT calculations were carried out with the three-parameter density functional (B3LYP) which includes Becke's gradient exchange correction[30] and the Lee, Young, and Parr correlation functional[31] using standard 6-311++G(d,p) basis set[32,33] and the Gaussian 03 program package[34] for neutral $FC(O)SCH_3$ in its ground state compute that the LUMO is a $\pi^*_{C=O}$ (a″) orbital with antibonding character. The next vacant orbitals correspond to the antibonding σ^*_{S-C} (SCH_3) (a′), σ^*_{S-C} (SC═O) (a′), and σ^*_{F-C} (a′). Three antibonding orbitals with similar energies attributed as σ^*_{C-H} localized in the CH_3-group and a $\sigma^*_{C=O}$ (a′) complete the antibonding molecular orbital representation expected for $FC(O)SCH_3$ (see Figure 1).

According to the UB3LYP/6-311++G (d, p) and B3LYP/6-311++G (d, p) method, the low-lying singly and doubly charged states are located at 10.0 and 27.0 eV above the neutral ground state, respectively. Both charged $FC(O)SCH_3^+$ and $FC(O)SCH_3^{2+}$ forms are stable minima in the low-lying cationic potential energy surfaces; i.e., no imaginary frequencies were found in the calculations. The planar skeleton of the $FC(O)SCH_3$ molecule remains unchanged after simple ionization, with a most important elongation of about 0.14 Å for the C−S single bond and the shortening of the other bond lengths. Bond angles in $FC(O)SCH_3^+$ are quite similar to those calculated for the neutral species. On the other hand, the most important structural difference between the neutral and the doubly charged ionic species is that the FC−SC dihedral angle changes from 180° in syn $FC(O)SCH_3$ to 85.2° in $FC(O)SCH_3^{2+}$ (almost in gauche orientation). When this species is compared with the neutral form, huge differences are observed in bond distances, bond angles, and torsions. After a double ionization the F−C single bond experiences an elongation of about 0.14 Å, while the C−S single bond is slightly longer than the same bond in the neutral form.

Total Ion Yield Spectra (TIY). The TIY spectra were obtained by recording the count rates of the total ions while the photon energy is scanned. At high photon energies corre-

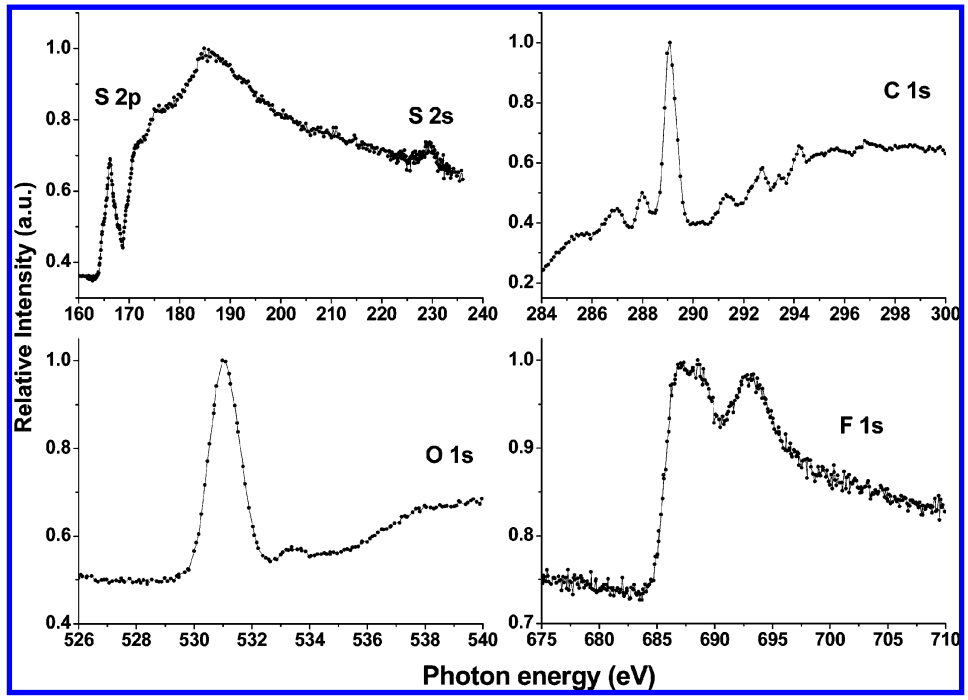

Figure 2. TIY spectra of $FC(O)SCH_3$ in the S 2p, C 1s, O 1s, and F 1s regions.

sponding to shallow- and core−shell electronic levels, the quantum yield for molecular ionization is quite likely tending to unity. Consequently, the detection of parent and fragment ions as a function of the incident photon energy is a powerful method to be used as a complement to the absorption spectroscopy.[35] The TIY spectrum of $FC(O)SCH_3$, measured near the S 2p edge is shown in Figure 2. Below the S 2p threshold (approximately 170.7 eV), the spectrum is dominated by an intense resonance centered at 166.2 eV and shoulders around 164.8, 167.1, and 168.0 eV. Two of these signals may correspond to transitions involving the spin−orbit split of the 2p term in the $2p_{1/2}$ and $2p_{3/2}$ levels in the excited species to unoccupied antibonding orbitals and in agreement with the $2J + 1$ rule; an intensity ratio of 1:2 is expected for these transitions. In the case of the simplest sulfide, H_2S, this splitting was reported to be 1.201 eV.[36] Superposed with the S 2p continuum a signal at 229.5 eV can be assigned to the S 2s edge (Figure 2).

As mentioned before, the lowest unoccupied orbital (LUMO) in $FC(O)SCH_3$ is a π^* orbital residing primarily at the carbonyl carbon and oxygen sites. Thus, it is expected that an intense $1s-\pi^*$ transition from the carbonyl carbon and the oxygen site would be observed. In the TIY spectrum measured near the C 1s region (Figure 2) the C 1s threshold is located at approximately 296.0 eV, and below this photon energy an intense signal at around 289.0 eV can be observed together with other low intense bands. Although two nonequivalent carbon atoms are present in $FC(O)SCH_3$, we were not able to assign the spectra from these different excitation sites. Probably, the strong signal at 289.0 eV is associated with the excitation of the 1s C (C═O) toward the vacant π^* antibonding, since the carbon atoms of the saturated hydrocarbons show mainly Rydberg transitions, which have in general lower intensities by an order of magnitude than π^* excitations.[37]

The TIY spectrum obtained near the O 1s region (Figure 2) is dominated by an intense resonance centered at 530.9 eV whereas the O 1s threshold is located at approximately 538.0 eV. A low-intensity signal was also observed at 533.6 eV. In this case, the O 1s $\rightarrow \pi^*$ (530.9 eV) transition dominates this region, and there are only small contributions from Rydberg transitions (as compared with the behavior of the C 1s region). Generally, the intensities of Rydberg transitions in the O 1s spectrum are weaker than the corresponding transitions in the C 1s spectrum, possibly because of the smaller spatial extent of the more tightly bound O 1s orbital and thus its poorer overlap with diffuse Rydberg orbitals. As has been reported for other carbonyl compounds,[38] electronic excitations to vacant antibonding $\pi^*_{C=O}$ and $\sigma^*_{C=O}$ orbitals may be associated with the signals observed at 530.9 and 533.6 eV, respectively. Finally, the TIY spectrum measured near the F 1s region (Figure 2) exhibits a broad signal centered at 687.0 eV. The ionization edge is located at approximately 693.0 eV.

PEPICO Spectra. Several PEPICO spectra taken at the most important S 2p, C 1s, O 1s, and F 1s transitions of $FC(O)SCH_3$ have been recorded in this work. In order to identify the role of resonant Auger processes in the fragmentation, spectra were measured not only at the resonant values (maxima of the absorptions) but also at photon energy values below (typically 10 eV) and above (typically 50 eV) each resonance. The PEPICO spectra measured for $FC(O)SCH_3$ at resonant S 2p, C 1s, O 1s, and F 1s edge absorptions are shown, together with a fragment assignment of the bands, in Figure 3. In Table 1 the corresponding branching ratios are collected for the main fragment ions.

The most intense peaks for the S 2p and S 2s energy ranges are observed for the HCS^+ ($m/z = 45$) and FCO^+ or H_3CS^+ ($m/z = 47$) ions with relative intensities between 13.5 and 17.0%. The next most abundant ions, are S^+ ($m/z = 32$) and H^+ ($m/z = 1$) reaching branching values of 11.5 and 10.9%, respectively. Other less abundant fragments are the following: the methyl fragments CH_x^+ ($x = 0, 1, 2, 3$) with $m/z = 12$, 13, 14, and 15, O^+ or S^{2+} ($m/z = 16$), F^+ ($m/z = 19$), CO^+ ($m/z = 28$), CF^+ ($m/z = 31$), SH^+ ($m/z = 33$), H_xCS^+ ($x = 0, 2$) with $m/z = 44$ and 46, FS^+ ($m/z = 51$), OCS^+ ($m/z = 60$), FCS^+ ($m/z = 63$), and $FSCH_3^+$ ($m/z = 66$). With respect to the last ion, it should be noted that methanesulfenyl fluoride, CH_3SF, has been observed in the broad band UV−visible irradiation of $FC(O)SCH_3$ isolated in a solid Ar matrix.[19] The $F + CH_3SSCH_3$

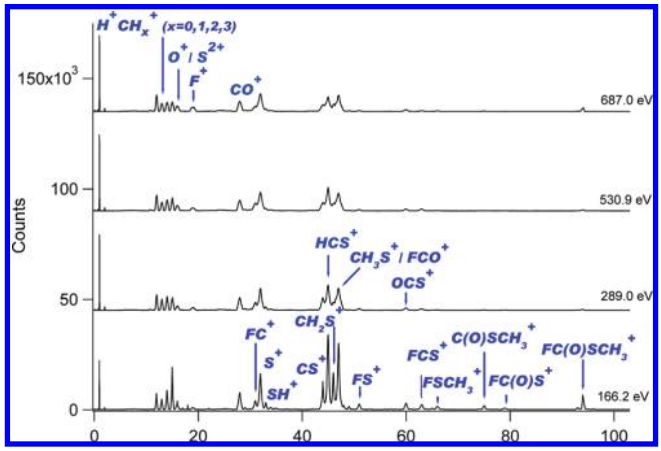

Figure 3. PEPICO spectra measured for $FC(O)SCH_3$ at resonant S 2p, C 1s, O 1s, and F 1s edge absorptions.

reaction has been also studied by He I photoelectron spectroscopy. This reaction proceeds via two competing routes, a hydrogen atom abstraction channel to generate the CH_3SSCH_2 radical, and an adduct channel, where the adduct unimolecularly decomposes to generate CH_3SF and CH_3S radical. A discharge-flow mass spectrometric study of $F + CH_3SCH_3$ was already performed. This reaction proceeds through two channels with formation of $CH_3SCH_2 + HF$ and $CH_3SF + CH_3$. In particular, the detection of a peak at $m/z = 66$ (CH_3SF^+) supports the existence of the last channel.[39]

Signals for the $COSCH_3^+$ ($m/z = 75$) and $FCOS^+$ ($m/z = 79$) ions also appear in these spectra, having weak relative intensity (1% approximately). It should be noted that only a singly charged molecular ion can produce $COSCH_3^+$ and $FCOS^+$ from ionized $FCOSCH_3$. In effect, even the whole remaining group F and CH_3 are lighter than $COSCH_3$ and FCOS and should be detected in the PEPICO spectra instead of $COSCH_3^+$ and $FCOS^+$. Thus, the detection of these ions in the PEPICO spectra implies the following mechanisms of dissociation

$$FC(O)SCH_3^+ \rightarrow F + C(O)SCH_3^+$$

$$FC(O)SCH_3^+ \rightarrow FCOS^+ + CH_3$$

The parent ion, $FC(O)SCH_3^+$, can be observed at $m/z = 94$ amu/q in all PEPICO spectra recorded at selected energies around the S 2p and S 2s absorption edges having relative intensities higher than 1% in the TOF mass spectra measured at photon energies near 166.2 and 170.7 eV. The low-intensity signal at 93 amu/q (<0.3%) indicates the presence of $FC(O)SCH_2^+$ ion.

More detailed information about the ion branched productions can be achieved form the partial ion yield (PIY) spectra for selected ions. In these PIY spectra, each point corresponds to one time-of-flight spectrum measured at this defined photon energy. The intensity of each ionic fragment is obtained by fitting a Gaussian function to the time-of-flight spectra. These spectra were normalized by the photon flux. Thus, PIY spectra were obtained in the 162−180 eV range by recording the count rates of selected ions while the photon energy is scanned in steps of 0.2 eV (Figure 4).

The intensity of the $m/z = 47$ amu/q ion signal corresponding to the ions FCO^+ and/or CH_3S^+ shows a steep enhancement at around the S 2p threshold. This signal becomes predominant at energies higher than 170.0 eV. Both ions can be formed by the rupture of the C−S bond involving the carbonyl carbon atom. Thus, a process involving excitations to the corresponding σ^*_{C-S} (SC═O) antibonding orbital can be suggested.

Partial ion yield spectra for selected $FC(O)SCH_3$ ions were also recorded around C 1s, O 1s, and F 1s ionization edges (Figures 5, 6, and 7). In all cases, the most intense peak in the PIY spectra is observed at m/z= 1 amu/q, corresponding to the H^+ ion. The PIY spectra for the main single charged ions simply mimic the TIY spectra.

The fragmentation pattern at the C 1s edge is dominated by signals appearing at 1 and 47 m/z ratios, which possess relative abundances higher than 15.9 and 12.0%, respectively. A second

TABLE 1: Branching Ratios (%) for Fragment Ions Extracted from PEPICO Spectra Taken at Photon Energies around the S 2p, S 2s, C 1s, O 1s, and F 1s Energies for $FC(O)SCH_3$

		branching ratios at various m/z values (amu/q)																				
electronic edge	photon energy (eV)	1 H^+	12 C^+	13 CH^+	14 CH_2^+	15 CH_3^+	16 O^+/S^{2+}	19 F^+	28 CO^+	31 CF^+	32 S^+	33 SH^+	44 CS^+	45 HCS^+	46 H_2CS^+	47 H_3CS^+/ FCO^+	51 FS^+	60 OCS^+	63 FCS^+	75 $COSCH_3^+$	79 $FC(O)S^+$	94 M^+
S 2p	166.2	5.8	3.5	2.8	4.3	6.7	2.1	1.4	5.0	2.3	8.2	1.6	4.3	17.0	6.8	15.8	1.6	1.8	1.9	1.1	1.0	2.3
	170.7	7.5	3.7	3.1	4.5	6.4	2.0	1.3	5.1	2.8	9.1	1.7	4.6	15.8	5.4	17.0	1.4	1.7	1.7			1.4
S 2s	215.0	10.6	4.7	3.3	4.9	7.0	2.1	1.3	6.0	2.9	11.3	1.4	3.7	14.0	4.6	16.0	1.0	1.4	1.1			
	225.9	10.9	5.0	3.5	4.9	6.8	2.2	1.4	6.2	3.0	11.5	1.3	3.7	13.5	4.5	15.8	1.0	1.3	1.0			
C 1s	279.0	16.3	6.2	4.2	5.6	7.2	3.1	2.1	6.3	3.7	11.1		3.0	9.4	1.6	16.2		1.1				
	286.9	15.9	6.5	4.6	6.5	7.1	3.3	3.0	6.6	3.7	11.0		3.2	8.1	1.6	14.5		1.0				
	288.1	16.4	6.6	4.6	6.0	6.1	3.1	2.8	6.7	3.7	10.8		4.3	9.9	1.8	13.2		1.0				
	289.0	16.0	6.3	4.6	6.0	5.8	2.7	2.0	6.6	3.8	11.3		4.8	11.5	2.0	12.6		1.0				
	291.2	16.5	7.6	4.5	5.7	6.2	4.8	2.8	7.3	3.8	10.7		4.0	8.5	1.6	12.3		1.0				
	292.7	16.8	6.9	4.5	6.1	6.4	3.7	3.0	7.3	3.6	10.8		3.7	8.8	1.5	12.8						
	294.3	17.7	6.9	4.8	6.2	6.0	3.2	2.9	7.3	3.8	11.1		4.1	8.7	1.4	12.0						
	339.0	19.0	7.2	4.7	5.7	6.0	3.3	2.5	6.8	3.7	11.7		3.3	8.2	1.2	12.7						
O 1s	521.0	20.0	8.4	4.6	5.5	5.4	4.6	3.7	6.9	3.7	11.0		3.3	7.1	1.3	10.9						
	530.9	17.7	7.3	4.4	5.7	5.9	3.6	2.6	6.2	4.1	11.3		3.7	10.9	1.9	10.7						
	533.6	19.7	7.9	4.6	5.7	5.6	3.9	2.8	6.6	3.8	11.9		3.3	8.0	1.3	11.3						
	581.0	19.2	8.7	4.4	5.3	5.3	5.9	3.2	7.0	3.8	10.7		3.3	7.2	1.5	10.7						
F 1s	677.0	19.5	9.0	4.3	5.0	5.1	5.8	2.9	6.4	3.6	10.7		3.2	7.6	1.8	11.0						
	687.0	19.2	8.2	4.6	5.5	5.3	4.1	4.0	6.6	3.2	11.7		3.4	8.1	1.9	10.0						
	693.0	19.4	8.4	4.5	5.5	5.3	4.7	4.0	7.0	3.2	11.8		3.2	7.6	1.7	9.7						
	737.0	19.0	9.0	4.3	5.5	4.9	5.9	5.3	7.3	3.0	10.9		3.1	6.9	1.6	9.4						

[a] Ions with branching ratios lower than 1.0% are not listed.

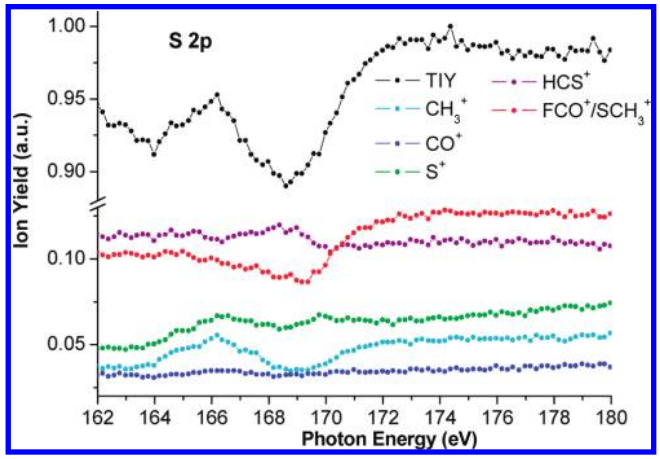

Figure 4. Partial ion yield spectrum for selected ions of $FC(O)SCH_3$ in the S 2p region.

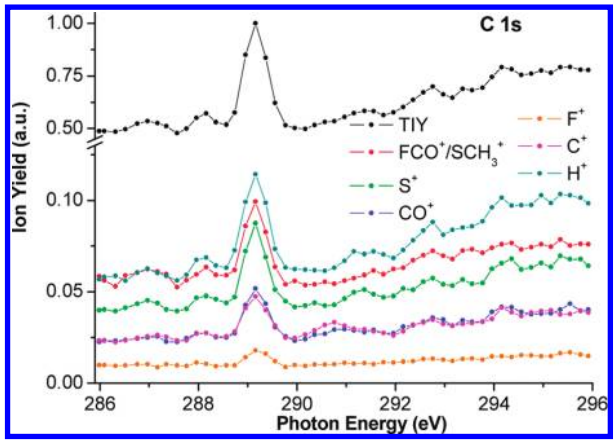

Figure 5. Partial ion yield spectrum for selected ions of $FC(O)SCH_3$ in the C 1s region.

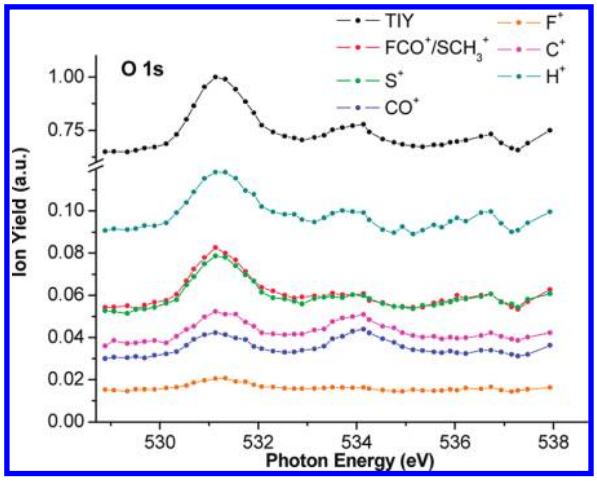

Figure 6. Partial ion yield spectrum for selected ions of $FC(O)SCH_3$ in the O 1s region.

group of less intense signals appears around $m/z = 32$ amu/q and $m/z = 45$ amu/q and shows important contributions between 8 and 11.7% approximately. Signals at 75 and 79 amu/q vanish when the photon energy reaches this value. Thus, at this high relative photon energy region processes involving singly charged ions are, as expected, less important than the doubly charged channels.

The fragmentation patterns at the O and F 1s edges seem to be basically identical. That is, the atomic hydrogen ion is again the most abundant fragment, followed by the signals at 32 (S^+) and 47 (FCO^+ or H_3CS^+) amu/q, respectively. The $m/z = 32$ amu/q signal intensity is similar or slightly more intense than the signal at $m/z = 47$ amu/q, evidence of a different behavior than that observed in the S 2p, S 2s, and C 1s regions, where the intensity of the S^+ ion is always lower. Surprisingly, the molecular ion at $m/z = 94$ amu/q can still be observed at these high energies as a very low-intensity signal (<1%).

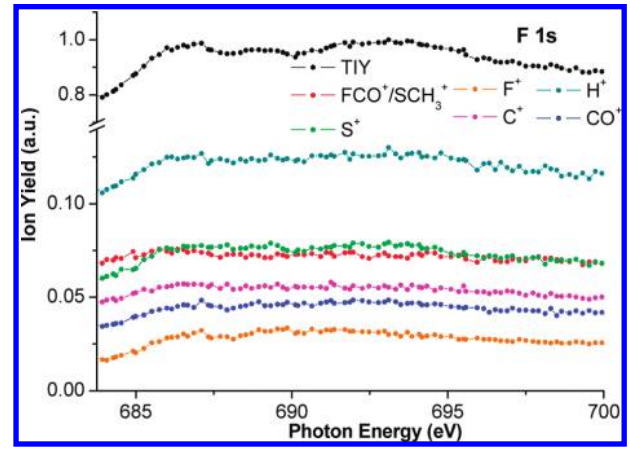

Figure 7. Partial ion yield spectrum for selected ions of $FC(O)SCH_3$ in the F 1s region.

In general, a clear enhancement in the intensity of the signal corresponding to the ion H^+ results is evident at increasing incident photon energies (from 6% near the S 2p edge to 20% near the F 1s edge). A small increment in the $m/z = 12$, 16, and 19 peak intensities, corresponding to the ions C^+, O^+/S^{2+}, and F^+, is observed by going toward higher energies. On the other hand, the intensity signals of the large ions at $m/z = 45$ (HCS^+) and 47 (FCO^+ or H_3CS^+) amu/q are depressed from 17 to 7% approximately by going from the S 2p to the F 1s region. This evidence can be related with the occurrence of a moderate site-specific fragmentation in $FC(O)SCH_3$.

Furthermore, the intensity of the signal corresponding to the CH_3^+ ion decreases slightly when the incident photon energy is increased. Together with this diminution an enhancement in the signal intensity of other methyl fragments ($CH_x^+ = 0, 1, 2$), in particular C^+ ion, can also be noticed by going from S 2p to the F 1s region.

PEPIPICO Spectra. It is well-known that core excitation and core ionization lead to resonant and normal Auger processes, which are highly effective electronic decay mechanisms in promoting the dissociation of molecules. The analysis of the PEPIPICO spectra is useful for identifying two-, three-, and four-body dissociation mechanisms which especially follow Auger decay processes.[40,41]

In the case of a rather complex molecule such as $FC(O)SCH_3$, several islands are expected in the PEPIPICO spectra and, hence, a complete interpretation of the spectra is not straightforward. As a first approximation, in the analysis of the PEPIPICO spectra, the following two aspects were taken into account. First, due to the inherent limited resolution used in the experiments, for islands involving m/z values of 16 and 47 amu/q, the distinction between O^+ and S^{2+} ions and FCO^+ and SCH_3^+ ions, respectively, is not always possible. Second, the peaks corresponding to double coincidences involving the m/z values of 1, 12, and 32 amu/q are the most intense signals, reflecting the importance of atomization processes in the dissociation mechanisms of $FC(O)SCH_3$. These processes may be originated by several multibody dissociation events that lead to the same final pair of atomic ions, making ambiguous the analysis of these

coincidences as appearing in the PEPIPICO spectra. Taking into consideration these facts, attention is paid to selected pairs of ions, for which both good statistics and well-defined shapes are observed. The double coincidence branching ratio for double ion processes calculated from PEPIPICO spectra at several photon energies around S 2p, C 1s, O 1s, and F 1s ionization edges is given in Table 2.

Two-body processes concerning the rupture of the C−S bond to form two single-charged species were observed as the main two-body dissociation channel in FC(O)SCl,[1] ClC(O)SCl,[3] $CH_3C(O)SH$,[4] and $CH_3OC(O)SCl$.[5] This channel emerges as general dissociation route for double-charged XC(O)SY species excited at inner shell levels. In this case, this fragmentation process leads to the formation of two ions with the same *m*/*z* value

$$FC(O)SCH_3^{2+} \rightarrow FCO^+ + CH_3S^+$$

The PEPIPICO spectra are limited onto the +1 slope, which prevent attempts to completely analyze the $FC(O)^+/SCH_3^+$ coincidence, as shown in Figure 8 (in PEPIPICO spectra the "aborted" half-peak at $FC(O)^+/SCH_3^+$ times can be noted). Moreover, the coincidence of the SCH_x^+ ($x = 0, 1, 2$) ions with the FCO^+ ion was also observed being the intensity of the island with $x = 1$ (HCS^+) was always higher than the others, reaching values of ca. 6.4, 8.9, 5.1, and 4.8% in the S 2p, C 1s, O 1s, and F 1s regions, respectively. The coincidence between FCO^+ and HCS^+ ions can be originated in a four-body secondary decay involving the rupture of the S−C (carbonylic carbon atom) bond in a first step, followed by the loss of neutral hydrogen atoms

$$FC(O)SCH_3^{2+} \rightarrow FCO^+ + CH_3S^+$$

$$CH_3S^+ \rightarrow CH_2S^+ + H$$

$$CH_2S^+ \rightarrow HCS^+ + H$$

The calculated slope of −0.96 is in relatively good agreement with the experimental value derived from the PEPIPICO spectra. For the study of the model involving the determination of the slopes in the PEPIPICO spectra and the connection with the fragmentation mechanisms, see refs 1−10 and the references cited therein.

A coincidence between CH_3^+ and FCO^+, with a maximum branching ratio of 5% at 166.2 eV, is observed with an experimental slope of −0.4, in very close agreement with the value of −0.32 predicted for the sequential step with an initial charge separation or secondary decay (SD) mechanism

$$FC(O)SCH_3^{2+} \rightarrow FCO^+ + SCH_3^+$$

$$SCH_3^+ \rightarrow S + CH_3^+$$

Coincidence spectra between the ions CH_2^+ and FCO^+ show a slight change in the slope when the loss of the hydrogen fragment increases. This fact might be evidence that the mechanisms involved in the formation of CH_2^+ ion can be sequential via the CH_3^+ ion formed in the very first step. Thus, four-body ion-pair processes need to be invoked to explain the coincidence between CH_2^+ and FCO^+ ions. Indeed little differences are expected in the slope of double coincidences involving CH_2^+ when compared with CH_3^+ because of the low mass of the hydrogen.

Fragmentation processes leading to the formation of S^+ and FCO^+ ions are observed as a very low intensity island in all energy ranges. The parallelogram-like shape of the island and the observed slope close to −0.6 can be explained by a by a secondary decay mechanism (the calculated slope is −0.68)

$$FC(O)SCH_3^{2+} \rightarrow FCO^+ + SCH_3^+$$

$$SCH_3^+ \rightarrow S^+ + CH_3$$

The coincidence between the CH_3^+ and S^+ ions, with a relative abundance of 6% at 166.2 eV (S 2p) and values of around 3% in the remaining energies with an experimental slope of −0.4 can be explained by a secondary decay mechanism

$$FC(O)SCH_3^{2+} \rightarrow FCOS^+ + CH_3^+$$

$$FCOS^+ \rightarrow S^+ + FCO$$

As much as 32% of the double coincidences that originated from $FC(O)SCH_3$ have the H^+ ion as the lightest ion in the spectrum recorded at 166.2 eV. This contribution increases when the photon energy is increased, accounting for 52% at 737.0 eV. Between others, the H^+/C^+ and H^+/S^+ are the most intense coincidences, followed in importance by the H^+/H_xCS^+ ($x = 0, 1$) pair of ions.

The HCS^+ Fragment from $FC(O)SCH_3$. One of the goals in the study of small covalent compounds is to collect and systematize enough information for the sake of comparison and examination. The analysis of the PEPICO spectra of $FC(O)SCH_3$ over the whole range of photon energies analyzed here reveals a preferential production of HCS^+ ions, while signals corresponding to ionic fragments CS^+ and H_2CS^+ appear as less intense bands (see Table 1). This ion has been also constantly observed in the ionic fragmentation of other sulfur compounds having a methyl group as $ClC(O)SCH_3$ and CH_3SCN.[6,10]

The thioformyl ion is fairly abundant in the interstellar medium and, in fact, was observed by Thaddeus et al. in 1981[42] before it was studied in the laboratory by Gudeman et al.[43] and later by Bogey et al.[44] On this subject, it is worth noting that HCS^+ is not only one of the more than 140 species recognized in the interstellar medium up to date but one of the key species to understand the interstellar sulfur chemistry. Its C═S bond is extremely strong[45,46] and the abundance ratio HCS^+/CS^+ observed in the interstellar medium[42,47] was found to be unusually higher than the theoretical predictions. This is due to its low recombination energy (charge transfer reactions are inhibited therefore) and the relatively large proton affinity of CS[48] which inhibits proton transfer from HCS^+ to most molecular species. Thus, HCS^+ is unreactive with all of the most abundant interstellar molecules and this is an important reason why it is readily detectable in interstellar clouds.[48,49] Moreover, in this and in our former studies using a wide range of photon radiation we can experimentally determine the stability of this ionic species not only through its thermal collisions with protons and ions but also due to its exposure to UV, X-ray, and cosmic radiation. This picture would need to be complemented, to use

TABLE 2: Relative Intensities for Double Coincidence Islands Derived from the PEPIPICO Spectra of $FC(O)SCH_3$ as a Function of the Photon Energy

coincidences		% partial double coincidence yield (PDCY)												
ion 1	ion 2	166.2 eV	279.0 eV	289.0 eV	291.2 eV	294.3 eV	339.0 eV	521.0 eV	530.98 eV	533.6 eV	581.0 eV	677.0 eV	687 eV	737.0 eV
H^+	C^+	4.8	8.0	9.2	12	9.7	9.4	11	9.5	10	10	12	12	12
H^+	CH^+	2.5	3.3	3.6	4.4	3.7	3.6	3.7	3.2	3.4	3.5	3.7	3.5	3.4
H^+	CH_2^+	1.3	1.8	1.7	1.9	1.8	1.7	1.6	1.5	1.6	1.5	1.6	1.5	1.5
H^+	O^+	1.2	2.7	3.0	3.8	3.1	3.1	4.1	3.6	3.9	4.0	5.0	4.8	5.0
H^+	F^+	0.75	2.0	2.3	2.4	2.3	2.3	3.1	2.6	2.8	2.7	3.3	3.6	3.9
H^+	CO^+	2.6	3.9	4.1	5.2	4.4	4.4	4.3	3.6	3.9	3.8	4.1	3.9	4.1
H^+	CF^+	1.2	2.1	2.2	2.5	2.4	2.3	2.4	2.2	2.1	2.4	2.6	2.3	2.2
H^+	S^+	7.6	9.2	10	13	10	10	10	9.5	10	9.7	11	11	11
H^+	SH^+	0.42												
H^+	CS^+	3.7	3.3	4.3	5.1	4.4	3.8	3.7	3.4	3.3	3.3	3.7	3.6	3.5
H^+	HCS^+	4.4	3.8	4.3	4.9	4.6	4.2	3.5	3.6	3.5	3.4	3.7	3.6	3.5
H^+	CH_2S^+	0.95	0.64	0.69	0.56	0.59	0.55	0.54	0.48	0.49	0.40	0.45	0.46	0.48
H^+	FCO^+	1.4	3.0	2.7	3.1	2.9	2.9	2.6	2.2	2.5	2.3	2.2	2.1	1.9
H_2^+	HCS^+	0.61	0.59	0.46	0.36	0.55	0.50	0.45	0.50	0.47	0.35	0.37	0.42	0.35
C^+	CH^+	0.42	0.47	0.42		0.36	0.47	0.47	0.62	0.55	0.56	0.41	0.57	0.48
C^+	CH_2^+	0.37	0.25	0.28			0.33	0.30	0.43	0.35	0.50	0.28	0.32	0.26
C^+	CH_3^+	0.37									0.38	0.22		0.29
C^+	O^+	1.1	0.89	0.95	2.0	1.0	1.1	2.5	1.7	1.8	3.1	3.9	2.1	3.9
C^+	F^+		0.47	0.52	0.31	0.47	0.62	1.0	1.0	1.1	0.95	0.89	1.2	1.2
C^+	CO^+	0.42	0.30	0.30	0.25		0.39	0.36	0.48	0.46	0.42	0.31	0.32	0.24
C^+	CF^+		0.29			0.31	0.30	0.43	0.47	0.43	0.52	0.41	0.42	0.32
C^+	S^+	3.3	3.7	4.0	3.8	3.6	4.0	4.1	4.0	4.1	3.6	4.3	4.4	4.2
C^+	CS^+	0.30		0.28			0.25	0.28	0.42	0.34	0.46	0.20	0.29	0.25
C^+	HCS^+	0.64		0.32			0.25		0.48	0.32		0.20	0.30	0.23
CH^+	O^+		0.32				0.26	0.34	0.48	0.41	0.50	0.29	0.36	0.29
CH^+	F^+							0.27	0.33	0.33	0.32		0.33	0.33
CH^+	CO^+	0.86	0.71	0.65		0.71	0.75	0.69	0.80	0.84	0.75	0.59	0.73	0.61
CH^+	CF^+	0.44	0.36	0.39	0.36	0.36	0.46	0.41	0.54	0.48	0.49		0.39	0.31
CH^+	S^+	3.4	2.8	3.1	2.4	2.8	2.9	2.7	2.7	2.8	2.4	2.5	2.8	2.6
CH^+	CS^+								0.32	0.24		0.37		
CH^+	FCO^+	0.57	0.44	0.30	0.28	0.36	0.42	0.35	0.44	0.43	0.53	0.28	0.28	
CH_2^+	O^+/S^{2+}		0.26				0.26	0.27	0.41	0.35		0.25		0.22
CH_2^+	F^+							0.30			0.38			0.45
CH_2^+	CO^+	1.6	1.1	1.2	0.77	1.2	1.2	1.0	1.2	1.2	0.87	0.83	1.1	1.1
CH_2^+	CF^+	0.79	0.62	0.64	0.42	0.62	0.56	0.60	0.80	0.66	0.60		0.53	0.43
CH_2^+	S^+	5.8	4.2	4.1	3.7	4.1	3.7	3.4	3.6	3.5	3.1	3.2	3.4	3.7
CH_2^+	SH^+	0.51												
CH_2^+	CS^+	0.52		0.27					0.34					
CH_2^+	FCO^+	2.2	1.6	1.5	1.1	1.4	1.5	1.3	1.3	1.3	1.3	1.1	1.0	0.94
CH_2^+	OCS^+	0.47												
CH_3^+	CO^+	1.8	0.82	0.64	0.37	0.62	0.68	0.63	0.79	0.74	0.67	0.44	0.66	0.82
CH_3^+	CF^+	0.86	0.51	0.42	0.33	0.44	0.41	0.44	0.61	0.52	0.46	0.36	0.37	0.26
CH_3^+	S^+	6.3	3.5	3.0	2.8	3.0	2.9	2.4	2.6	2.6	2.4	2.4	2.6	2.6
CH_3^+	CS^+	0.38												
CH_3^+	FCO^+	5.0	4.9	3.7	4.4	3.8	3.4	2.8	2.4	2.7	2.5	2.3	2.1	1.8
CH_3^+	SF^+	0.86	1.00	0.60	0.62	0.59	0.64	0.43	0.46	0.50	0.40	0.28	0.30	
CH_3^+	OCS^+	1.9	1.1	0.91	0.58	0.98	0.78	0.62	0.64	0.65	0.58	0.50	0.92	0.52
CH_3^+	FCS^+	0.55												
S^{2+}	CO^+	0.56			0.57			0.34			1.3	0.98		1.1
O^+/S^{2+}	CF^+		0.25					0.30	0.43	0.37	0.46	0.24	0.28	0.21
O^+	S^+	0.63	0.95	0.83	0.57	0.77	1.1	1.1	1.4	1.4	1.1	1.2	1.5	1.3
O^+	CS^+			0.26				0.27	0.40		0.38	0.25	0.32	0.24
F^+	CO^+					0.29		0.42		0.34	0.39			0.66
F^+	S^+	0.41	0.50	0.46		0.33	0.57	0.67	0.87	0.87	0.72	0.59	1.00	0.96
CO^+	S^+	2.9	2.7	2.4	2.2	2.5	2.7	2.5	2.4	2.6	2.0	2.3	2.4	2.3
CO^+	CS^+	0.61	0.41	0.53	0.31		0.48	0.55	0.59	0.48	0.55	0.40	0.47	0.45
CO^+	HCS^+	4.5	2.3	2.9	2.0	2.8	2.5	2.1	2.5	2.2	2.2	2.1	2.4	2.5
CO^+	CH_2S^+	1.2												
CO^+	CH_3S^+	0.59												
CF^+	S^+	0.40	0.55	0.44	0.31	0.38	0.51	0.47	0.70	0.64	0.55	0.47	0.48	0.33
CF^+	HCS^+	1.0	0.75	0.86	0.39	0.79	0.80	0.65	1.1	0.78	0.79	0.68	0.63	0.48
S^+	FCO^+	1.2	1.8	1.0	0.78	0.92	1.4	1.1	1.3	1.4	1.0	0.78	0.77	0.51
CS^+	FCO^+	0.43	0.65	0.70	0.69	0.84	0.68	0.75	0.65	0.66	0.80	0.41	0.49	0.29
HCS^+	FCO^+	6.4	8.9	7.8	8.3	7.3	6.8	5.0	4.8	5.1	4.8	4.8	4.4	3.8
CH_2S^+	FCO^+	1.8	0.55	0.44	0.33	0.29	0.36	0.30	0.29	0.30	0.19	0.20	0.23	0.14

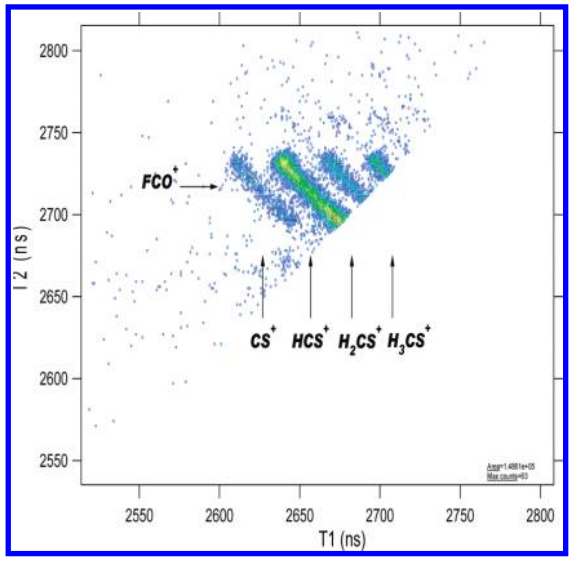

Figure 8. Enlargement of the PEPIPICO spectrum of $FC(O)SCH_3$ obtained at 166.2 eV photon energy in the range of m/z 44−47 amu/q in the T1 and T2 domains.

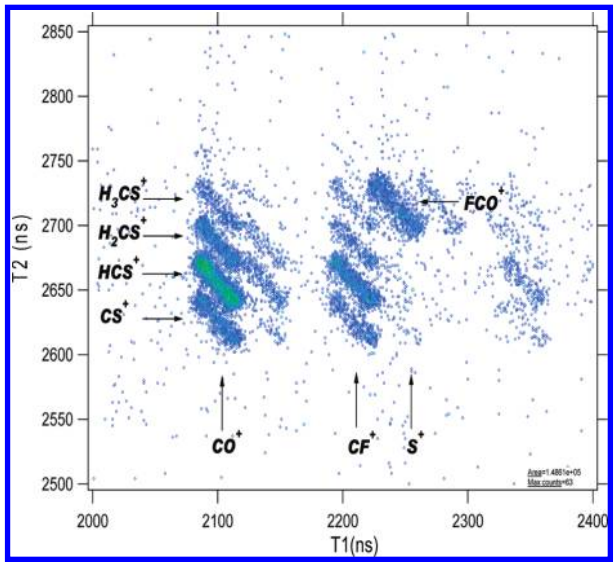

Figure 9. Enlargement of the PEPIPICO spectrum of $FC(O)SCH_3$ obtained at 166.2 eV photon energy in the ranges of m/z 28−32 and 44−47 amu/q in the T1 and T2 domains, respectively.

a more complete interstellar medium model, with the inclusion of very small dust grains which enables a further surface chemistry of molecules and ions. However, a part of the chemical or photochemical conditions of the molecular clouds characterized by low temperature and pressures are reproduced in our experiences using the synchrotron facility.

It is also important to notice the contribution of the HCS^+ ion to the double coincidence spectra. As we mentioned before, the high stability of the HCS^+ precludes subsequent dissociation of this ion (see Figure 8 discussed before). Thus, the coincidences involving this fragment are observed at all the photon energies studied with larger relative intensity than the double coincidence concerning the other ions corresponding to the series CH_xS^+ ($x = 0, 2, 3$). In effect, the analysis of PEPIPICO spectra reveals the presence of strong-intensity islands for the HCS^+ ions in coincidence with those arriving at times corresponding to $m/z = 28$ amu/q (CO^+) ions (Figure 9). This coincidence, with a relative abundance of 4.5% at 166.2 eV and values of around 2% in the remaining energies, with an experimental slope close to −1.0 can be explained by a deferred charge separation four-body ion process.

Conclusion

Small molecular species containing different kind of atoms give origin to interesting physicochemical processes which can be analyzed using the synchrotron facilities. A moderate site-specific fragmentation has been observed for the title molecule. This molecule gives origin to the stable interstellar HCS^+ ion in the same way as several other species relevant in the literature. A comparison of the CH_xS^+ ($x = 0-3$) islands, for instance, appearing in different PEPIPICO spectra confirms the high stability of the HCS^+ species, now formed under synchrotron conditions.

Acknowledgment. This work has been largely supported by the Brazilian Synchrotron Light Source (LNLS). The authors wish to thank Arnaldo Naves de Brito and his research group for fruitful discussions and generous collaboration during their several stays in Campinas and the TGM and SGM beamline staffs for their assistance throughout the experiments. They also are indebt to the Agencia Nacional de Promoción Científica y Tecnológica (ANPCyT), Consejo Nacional de Investigaciones Científicas y Técnicas (CONICET), and the Comisión de Investigaciones Científicas de la Provincia de Buenos Aires (CIC), República Argentina, for financial support. They also thank the Facultad de Ciencias Exactas, Universidad Nacional de La Plata, República Argentina for financial support. C.O.D.V. especially acknowledges the DAAD, which generously sponsors the DAAD Regional Program of Chemistry for the República Argentina supporting Latin American students who earn their PhD in La Plata.

References and Notes

(1) Erben, M. F.; Romano, R. M.; Della Védova, C. O. *J. Phys. Chem. A* **2004**, *108*, 3938.
(2) Geronés, M.; Erben, M. F.; Romano, R. M.; Della Védova, C. O. *J. Electron Spectrosc. Relat. Phenom.* **2007**, *155*, 64.
(3) Erben, M. F.; Romano, R. M.; Della Védova, C. O. *J. Phys. Chem. A* **2005**, *109*, 304.
(4) Erben, M. F.; Geronés, M.; Romano, R. M.; Della Védova, C. O. *J. Phys. Chem. A* **2006**, *110*, 875.
(5) Erben, M. F.; Geronés, M.; Romano, R. M.; Della Védova, C. O. *J. Phys. Chem. A* **2007**, *111*, 8062.
(6) Cortés, E.; Erben, M. F.; Geronés, M.; Romano, R. M.; Della Védova, C. O. *J. Phys. Chem. A* **2009**, *113*, 564.
(7) Cortés, E.; Erben, M. F.; Geronés, M.; Romano, R. M.; Della Védova, C. O. *J. Phys. Chem. A* **2009**, *113*, 9624.
(8) Geronés, M.; Erben, M. F.; Romano, R. M.; Della Védova, C. O.; Yao, L.; Ge, M. *J. Phys. Chem. A* **2008**, *112*, 2228.
(9) Geronés, M.; Downs, A. J.; Erben, M. F.; Ge, M.; Romano, R. M.; Yao, L.; Della Védova, C. O. *J. Phys. Chem. A* **2008**, *112*, 5947.
(10) Geronés, M.; Erben, M. F.; Ge, M.; Cavasso Filho, R. L.; Romano, R. M.; Della Védova, C. O. *J. Phys. Chem. A*, in press.
(11) Eberhardt, W.; Sham, T. K.; Carr, R.; Krummacher, S.; Strongin, M.; Weng, S. L.; Wesner, D. *Phys. Rev. Lett.* **1983**, *50*, 1038.
(12) Erman, P.; Karawajczyk, A.; Rachlew, E.; Stankiewicz, M.; Yoshiki Franzen, K. *J. Chem. Phys.* **1997**, *107*, 10827.
(13) Hanson, D. M. *Adv. Chem. Phys.* **1990**, *77*, 1.
(14) Mueller-Dethlefs, K.; Sander, M.; Chewter, L. A.; Schlag, E. W. *J. Phys. Chem.* **1984**, *88*, 6098.
(15) Miron, C.; Simon, M.; Leclercq, N.; Hansen, D. L.; Morin, P. *Phys. Rev. Lett.* **1998**, *81*, 4104.
(16) Boo, B. H.; Saito, N. *J. Electron Spectrosc. Relat. Phenom.* **2003**, *128*, 119.
(17) Caminati, W.; Meyer, R. *J. Mol. Spectrosc.* **1981**, *90*, 303.
(18) Della Védova, C. O. *J. Raman Spectrosc.* **1989**, *20*, 483.
(19) Romano, R. M.; Della Védova, C. O.; Downs, A. J. *Chem.—Eur. J.* **2007**, *13*, 8185.
(20) Lira, A. C.; Rodrigues, A. R. D.; Rosa, A.; Goncüalves da Silva, C. E. T.; Pardine, C.; Scorzato, C.; Wisnivesky, D.; Rafael, F.; Franco, G. S.; Tosin, G.; Lin, L.; Jahnel, L.; Ferreira, M. J.; Tavares, P. F.; Farias,

R. H. A.; Neuenschwander, R. T. First Year Operation of the Brazilian Sinchrotron Light Source In *EPAC98, European Particle Accelerator Conference, Stockholm*; Institute of Physics: London, 1998.

(21) Craievich, A. F.; Rodrigues, A. R. *Hyperfine Interact.* **1998**, *113*, 465.

(22) Rodrigues, A. R. D.; Craievich, A. F.; Gonçalves da Silva, C. E. T. *J. Synchrotron Radiat.* **1998**, *5*, 1157.

(23) Cavasso Filho, R. L.; Homen, M. G. P.; Fonseca, P. T.; Naves de Brito, A. *Rev. Sci. Instrum.* **2007**, *78*, 115104.

(24) Cavasso Filho, R. L.; Lago, A. F.; Homem, M. G. P.; Pilling, S.; Naves de Brito, A. *J. Electron Spectrosc. Relat. Phenom.* **2007**, *156*−*158*, 168.

(25) de Fonseca, P. T.; Pacheco, J. G.; Samogin, E.; de Castro, A. R. B. *Rev. Sci. Instrum.* **1992**, *63*, 1256.

(26) Frasinski, L. J.; Stankiewicz, M.; Randall, K. J.; Hatherly, P. A.; Codling, K. *J. Phys. B: At. Mol. Phys.* **1986**, *19*, L819.

(27) Eland, J. H. D.; Wort, F. S.; Royds, R. N. *J. Electron Spectrosc. Relat. Phenom.* **1986**, *41*, 297.

(28) Burmeister, F.; Coutinho, L. H.; Marinho, R. R. T.; Homem, M. G. P.; de Morais, M. A. A.; Mocellin, A.; Björneholm, O.; Sorensen, S. L.; Fonseca, P. T.; Lindgren, A.; Naves de Brito, A. *J. Electron Spectrosc. Relat. Phenom.* **2010**, *180*, 6.

(29) Naves de Brito, A.; Feifel, R.; Mocellin, A.; Machado, A. B.; Sundin, S.; Hjelte, I.; Sorensen, S. L.; Bjorneholm, O. *Chem. Phys. Lett.* **1999**, *309*, 377.

(30) Becke, A. D. *Phys. Rev. A* **1988**, *38*, 3098.

(31) Lee, C. T.; Yang, W. T.; Parr, R. G. *Phys. Rev. B* **1988**, *37*, 785.

(32) Frisch, M. J.; Pople, J. A.; Binkley, J. S. *J. Chem. Phys.* **1984**, *80*, 3265.

(33) Clark, T.; Chandrasekhar, J.; Spitznagel, G. W.; Schleyer, P. v. R. *J. Comput. Chem.* **1983**, *4*, 294.

(34) Frisch, M. J.; Trucks, G. W.; Schlegel, H. B.; Scuseria, G. E.; Robb, M. A.; Cheeseman, J. R.; Montgomery, J. A., Jr.; Vreven, T.; Kudin, K. N.; Burant, J. C.; Millam, J. M.; Iyengar, S. S.; Tomasi, J.; Barone, V.; Mennucci, B.; Cossi, M.; Scalmani, G.; Rega, N.; Petersson, G. A.; Nakatsuji, H.; Hada, M.; Ehara, M.; Toyota, K.; Fukuda, R.; Hasegawa, J.; Ishida, M.; Nakajima, T.; Honda, Y.; Kitao, O.; Nakai, H.; Klene, M.; Li, X.; Knox, J. E.; Hratchian, H. P.; Cross, J. B.; Adamo, C.; Jaramillo, J.; Gomperts, R.; Stratmann, R. E.; Yazyev, O.; Austin, A. J.; Cammi, R.; Pomelli, C.; Ochterski, J. W.; Ayala, P. Y.; Morokuma, K.; Voth, G. A.; Salvador, P.; Dannenberg, J. J.; Zakrzewski, V. G.; Dapprich, S.; Daniels, A. D.; Strain, M. C.; Farkas, O.; Malick, D. K.; Rabuck, A. D.; Raghavachari, K.; Foresman, J. B.; Ortiz, J. V.; Cui, Q.; Baboul, A. G.; Clifford, S.; Cioslowski, J.; Stefanov, B. B.; Liu, G.; Liashenko, A.; Piskorz, P.; Komaromi, I.; Martin, R. L.; Fox, D. J.; Keith, T.; Al-Laham, M. A.; Peng, C. Y.; Nanayakkara, A.; Challacombe, M.; Gill, P. M. W.; Johnson, B.; Chen, W.; Wong, M. W.; Gonzalez, C.; Pople, J. A. *GAUSSIAN 03 (Revision B.5)*; Gaussian, Inc.: Wallingford, CT, 2004.

(35) Nenner, I.; Beswick, J. A. Molecular Photodissociation and Photoionization. In *Handbook on Synchrotron Radiation*; Marr, G. V., Ed.; Elsevier Science Publishers: Amsterdam, 1987; Vol. 2, pp 355−462.

(36) Svensson, S.; Naves de Brito, A.; Keane, M. P.; Correia, N.; Karlsson, L. *Phys. Rev. A* **1991**, *43*, 6441.

(37) Eberhardt, W.; Haelbich, R. P.; Iwan, M.; Koch, E. E.; Kunz, C. *Chem. Phys. Lett.* **1976**, *40*, 180.

(38) Lessard, R.; Cuny, J.; Cooper, G.; Hitchcock, A. P. *Chem. Phys.* **2007**, *331*, 289.

(39) (a) Baked, J.; Dyke, J. M. *J. Phys. Chem.* **1994**, *98*, 751. (b) Butkovskaya, N. I.; Poulet, G.; LeBras, G. *J. Phys. Chem.* **1995**, *99*, 4536.

(40) Eland, J. H. *Mol. Phys.* **1987**, *61*, 725.

(41) Simon, M.; Lebrun, T.; Martins, R.; de Souza, G. G. B.; Nenner, I.; Lavollee, M.; Morin, P. *J. Phys. Chem.* **1993**, *97*, 5228.

(42) Thaddeus, M.; Linke, R. A. *Astrophys. J.* **1981**, *246*, L41.

(43) Gudeman, C. S.; Haese, N. N.; Piltch, N. D.; Woods, R. C. *Astrophys. J.* **1981**, *246*, L47.

(44) Bogey, M.; Demuynck, C.; Destombes, J. L.; Lemoine, B. *J. Mol. Spectrosc.* **1984**, *107*, 417.

(45) Margulés, L.; Lewen, F.; Winnewisser, G.; Botschwina, P.; Müller, H. S. P. *Phys. Chem. Chem. Phys.* **2003**, *5*, 2770.

(46) Puzzarini, C. *J. Chem. Phys.* **2005**, *123*, 24313.

(47) Hirahara, Y.; Susuki, H.; Yamamoto, S.; Kawaguchi, K.; Karfu, N.; Chishi, M.; Takano, S.; Ishikawa, S. I.; Masuda, A. *Astrophys. J.* **1992**, *394*, 539.

(48) Smith, D.; Adams, N. G. *J. Phys. Chem.* **1985**, *89*, 3964.

(49) Smith, D. *Chem. Rev.* **1992**, *92*, 1473.

JP1081164